Journal of Environmental Engineering and Energy

www.jeee.reapress.com

J. Environ. Eng. Energy Vol. 2, No. 1 (2025) 64–75.

Paper Type: Original Article

Numerical Optimization and Analysis of Pressure Drop in Industrial Basket Strainers for Diesel and Water Flows

Seyed Mahmood Kia[1,*], Seyed Ahmad Kia[2]

[1] Department of Mechanical & Energy Engineering, Shahid Beheshti University, Tehran, Iran; mahmoud.kia.73@gmail.com.

[2] Department of Environmental and Mechanical Engineering, University of Guelph, Ontario, Canada; ahmadkia.68@gmail.com.

Citation:

Received: 18 September 2024 *Revised: 12 November 2024* *Accepted: 14 January 2025*	Kia, S. M., & Kia, S. A. (2025). Numerical optimization and analysis of pressure drop in industrial basket strainers for diesel and water flows. *Journal of environmental engineering and energy, 2*(1), 64-75.

Abstract

This paper analyzes the fluid dynamics and corresponding pressure loss within industrial hydraulic filtration mechanisms, with a special focus on basket strainers used for diesel and water flows. Hydraulic systems inevitably accumulate contaminants such as dust, sand, and metal particles that lower the efficiency of operations and cause accelerated equipment wear. Therefore, effective filtration is an absolute requirement for maintaining fluid cleanliness, extending machine life, and ensuring system reliability. In this respect, the work tries to optimize filtration efficiency by showing the effects of different inlet pressures and fluid properties at various operating conditions. One could see that for diesel, as the inlet pressure increases from 0.6 to 20 bar, the pressure drop leaps from 5.2 to 166 psi, and the flow rate rises from 3014 to 18163 GPM since diesel has higher viscosity and hence inherent opposition. The water flow shows similar trends with smaller pressure drops; for example, at 5000 GPM, the pressure drop in this case is 11.24 psi due to the lower viscosity of water. In both fluids, flows change from laminar to turbulent with increased rates, further increasing the frictional resistance and pressure drop. Model validation against empirical data showed a strong correlation, with an error margin of around 10%, thus showing that it was correct and exact in making predictions concerning fluid flow behavior in industrial filters. These results are significant in reaching optimal filtration system designs and in the continuous monitoring of pressure drops to enhance efficiency and prolong life under various conditions. In this manner, it contributes fundamental knowledge to the advancement of hydraulic filtration for industrial applications.

Keywords: Basket strainers, Computational fluid dynamics, Pressure drop, Filtration systems.

1 | Introduction

Optimal fluid quality is one of the backbones to surmounting operational hurdles and improving efficiency and reliability in hydraulic systems. Although detailed system-filling and servicing protocols play a critical role in maintaining fluid cleanliness, such measures alone are insufficient to ensure optimal performance. Filters

Corresponding Author: mahmoud.kia.73@gmail.com

https://doi.org/10.22105/jeee.v2i1.34

and strainers are essential for protecting hydraulic systems by continuously removing contaminants, thereby preserving fluid integrity. Hydraulic fluid cleanliness is critical to the long-term functioning of any system. Hydraulic systems can accumulate a wide range of contaminants during operation, including air, water, lubricating oils, greases, pipe joint compounds, coolants, dust, sand, and metal particles. More complex contaminants include resins, acids, gums, varnishes, machining debris, and sludge. If not properly managed, these impurities can cause extensive wear on system components, resulting in problems such as valve sticking, seal leakage, and reduced performance.

Therefore, it is essential to remove contaminants effectively to maintain the durability and operational effectiveness of hydraulic systems. Settling, filtration, and magnetic separation are common methods used to remove contaminants. Although chemical additives can enhance the performance characteristics of fluids, such substances do not eliminate impurities, making filtration a critical process. Further, basket strainers provide a strong mechanical filtration method by capturing contaminants and improving flow quality. In this context, basket strainers play a vital role in the flow dynamics regulation and reduction of pressure drops.

In this context, basket strainers are crucial for regulating flow dynamics and minimizing pressure drops. These components are designed to manage the flow dynamics efficiently while reducing pressure losses. Recent developments in the optimization of thermodynamic and fluid dynamic principles have increased the understanding of energy efficiency and the reliability of the systems. Research has pointed out the potential of other alternative methodologies, such as the use of advanced cooling agents like ammonia and waste heat recovery technologies, to enhance thermal efficiency while at the same time being able to reduce environmental impacts [1], [2].

Such innovative strategies, of course, open up new dimensions in integrating sustainable energy systems into industrial applications, leading toward reduced energy losses and enhanced sustainability of operations [3]. These technologies are aligned with the goals of increasing filtration efficiency and prolonging the operational life of hydraulic systems. The design parameters, including the configuration of outlet perforation and the flow pattern analysis, directly influence both the outlet pressure and heat transfer efficiency. Various studies have indicated that the changes in flow patterns can appreciably influence the pressure oscillations and heat transfer characteristics in such systems [4–6].

Progress in sustainable energy systems is central to meeting global energy needs and stabilizing climate change. Carbon Capture and Storage (CCS) technologies are increasingly recognized as essential in mitigating industrial CO_2 emissions [7]. The integration of renewable energy systems, such as photovoltaic-powered double-effect absorption chillers, further reduces reliance on fossil fuels while improving energy efficiency [8], [9]. Efforts to identify environmentally friendly industrial solutions have also explored biodiesel production from Kolanut oil and the use of natural corrosion inhibitors, such as avocado seed oil [10], [11].

In the field of drip irrigation, pressurized granular bed filters have demonstrated non-uniform flow regions and elevated Reynolds numbers near underdrain slots, leading to deviations in predicted pressure drops when compared to conventional packed bed correlations. The commonly used equations, such as those by Ergun, Darcy-Forchheimer, and Kozeny-Carman, show different degrees of accuracy based on the conditions of the flow. In fact, according to Computational Fluid Dynamics (CFD) simulations, especially in the case of high flow rates, the Ergun equation gives satisfactory predictions for materials like silica sand. This underlines the importance of accurate modeling to improve both filter efficiency and energy efficiency [12].

Other research in hydraulic filtration systems has focused on complex flow dynamics and corresponding pressure losses. Korkmaz et al. [13] performed experimental and numerical flow and pressure drop analyses of the hydraulic filters for Reynolds numbers in the range 1250–2350. They showed that fluid flow over the filter surfaces is mainly non-uniform. The leading pressure drops are found to be stemming from the Dean vortex at the outlet, thus providing a better understanding of contaminant accumulation and pressure drop mechanisms. Filtration studies are not only limited to hydraulic systems but also to more general industrial applications. Brazhenko et al. [14] reported dynamic rotating perforated cylinder filters for hydraulic oil

filtration and showed effective contaminant removal through experiments and CFD analysis. Their work pointed out the role of vortex flows in reducing membrane fouling, leading to increased filtration efficiency over time.

Similarly, Klarecki and Rabsztyn [15] included filter efficiency by comparing mathematical models to experimental tests, showing the effect of flushing time and particle concentration on filtration performance. Tič and Lovrec [16] analyzed the connection of pressure drop development with online condition monitoring in hydraulic filters. Their study has shown that an impurity accumulation increases resistance within return-line filters; therefore, clogging indicators and bypass mechanisms may be activated. Effective pressure monitoring is crucial for ensuring system reliability and maintaining operational stability.

Gorle et al. [17] experimentally proved the influence of oil temperature, flow rate, and contamination levels on hydraulic filter performance and showed that a higher oil temperature decreases viscosity, slowing down the buildup of pressure drop, while greater contamination hastens clogging. Serone's work on basket strainers used computational modeling and experimental analysis to show the effects of changes in inlet pressures on filtration efficiency for diesel and water flows.

The results indicated that optimized strainer design and continuous monitoring significantly improved efficiency, reduced wear, and assured reliable system performance under a variety of conditions [18]. Gaj's [19] study on the structural behavior of perforated corrugated High-Density Polyethylene (HDPE) drainage pipes, utilizing finite-element modeling, revealed that perforations significantly amplify stress concentrations and increase the likelihood of failure at shallow depths. This underscores the importance of considering perforation characteristics to enhance the performance of drainage systems.

Mahajan et al. [20] used CFD tools to optimize the performance of T-type strainers. They introduced the design modifications by changing the punch plate size and the inlet-outlet configurations that could significantly reduce the pressure losses and improve overall efficiency. Similarly, Neihguk et al. [21] treated the perforated pipes as a part of concentric tube resonators to demonstrate how geometric variations affect flow dynamics and pressure drop; they also provided instructive information concerning automotive muffler system design.

Azadi et al. [22] developed a three-dimensional reservoir-wellbore model using CFD to analyze flow in perforated pipes surrounded by porous media. Their findings have shown that factors such as perforation density, diameter, and phasing angle affect wall friction and pressure loss, thus guiding optimization of the design for production wellbores.

Dehghan Afifi et al. [23] emphasize that optimizing fluid quality is fundamental to overcoming operational challenges and enhancing the efficiency and reliability of hydraulic systems. They further underscore that while following system-filling and servicing protocols is essential to maintain fluid cleanliness, these measures alone are inadequate for ensuring peak performance. In line with this, the research points out that various filtration and separation techniques, including magnetic separation and basket strainers, play a vital role in sustaining fluid integrity by continuously removing contaminants.

Additionally, studies in this domain have explored novel methodologies and technological advancements aimed at improving filtration efficiency, energy management, and system sustainability. These innovations, such as advanced cooling agents, heat recovery systems, and renewable energy integrations, contribute to the broader goals of increasing the operational lifespan of hydraulic systems while mitigating environmental impacts. Furthermore, ongoing studies into complex flow dynamics and pressure drop mechanisms in hydraulic filtration systems continue to provide valuable insights.

Furthermore, similar investigations have been carried out in various industries, demonstrating a growing interest in optimizing filtration systems for both performance and environmental sustainability. Furthermore, other related research in this field also exists [24–27].

Based on this vast amount of research, the current study focuses on numerical modeling and analysis of fluid dynamics and pressure loss in basket strainers used in industrial hydraulic filtration systems. This work examines the dynamics of flows of diesel and water, focusing on the effects of inlet pressures, flow rates, and fluid properties on filtration efficiency. Computational models, validated against experimental data, highlight the importance of properly designed strainers in reducing energy losses, enhancing system longevity, and enabling proper performance over a wide range of conditions.

2 | Governing Equation

The basis of the modeling of fluid flow through basket strainers was founded on fundamental principles of fluid mechanics, with the continuity equation dealing with mass conservation and the momentum equation (Navier-Stokes) defining the forces acting on the fluid. The continuity equation, expressed in *Eq. (1)*, ensures mass conservation through its flowing in and out of a defined control volume over a given period:

$$\frac{\partial \rho}{\partial t} + \nabla.(\rho u) = 0, \quad (1)$$

where ρ is the fluid density, and u is the velocity vector, which together quantifies the speed and direction of fluid flowing in the system. The momentum equation, derived from Newton's second law and also referred to as the Navier-Stokes equation *Eq. (2)*, is a description of the forces that act on the fluid, where inertial forces are balanced by pressure, viscous, and external forces:

$$\rho\left(\frac{\partial u}{\partial t} + u.\nabla u\right) = -\nabla p + \mu\nabla^2 u + f, \quad (2)$$

where p is the pressure, μ is the dynamic viscosity responsible for the resistance, and f represents external forces, which include gravity. The pressure gradient term ($-\nabla p$) influences the acceleration of fluid, while the viscous term ($\mu\,\nabla^2 u$) represents internal friction. To precisely simulate fluid flow through a basket strainer, it is essential to establish appropriate boundary conditions.

The no-slip boundary condition dictates that the fluid velocity at the strainer's surface must be zero. In turbulent flows, the shear stress (τ), representing the frictional resistance between fluid layers, is defined by *Eq. (3)*:

$$\tau = \mu\frac{\partial u}{\partial y}. \quad (3)$$

In *Eq. (3)*, ($\partial u/\partial y$) denotes the velocity gradient perpendicular to the flow direction, explaining the change in the flow velocity between adjacent layers and being directly responsible for the pressure drop. To determine the regime of flow, the Reynolds number defined by *Eq. (4)* is used.

The flow regime is determined using the Reynolds number, as defined by *Eq. (4)*. This dimensionless value indicates whether the flow is laminar or turbulent; the flow becomes turbulent when the Reynolds number crosses an inherent critical value.

$$Re = \frac{\rho V L}{\mu}. \quad (4)$$

In this equation, V is the velocity, L is the characteristic length, and μ is the dynamic viscosity. To account for the additional stresses due to turbulent eddies under conditions of turbulent flow, models like k- ε are used. The basket strainer's pressure drop and flow rate are studied numerically using finite element analysis-FEA or finite volume methods -FVM. The flow rate (Q), or the volume of fluid passing an area in a given time, is mathematically expressed by *Eq. (5)*:

$$Q = A \times V, \quad (5)$$

where A is the cross-sectional area, and V is the fluid velocity. When the cross-sectional area is constant, an increase in flow rate leads to higher velocity, resulting in a greater pressure drop.

The Darcy-Weisbach equation predicts the head loss due to friction (hf) as indicated in *Eq. (6)*:

$$h_f = f\frac{L}{D}\frac{v^2}{2g}, \quad (6)$$

where f is the friction factor, L is the length of the pipe, D is the diameter of the pipe, V is the velocity of the fluid, and g is the acceleration due to gravity. This head loss is directly adding to the pressure drop (ΔP), which is estimated in *Eq. (7)*:

$$\Delta P = \gamma \times h_f, \quad (7)$$

where γ is the weight of the fluid per unit volume. As seen from *Eq. (7)*, increased head loss by way of increased velocities will translate to an equivalent increased pressure drop, which agrees with theoretical prediction and could be taken as a verification of the precision of the model in simulating the fluid dynamics in industrial strainers.

3 | Numerical Modeling

Accurate modeling of such complex fluid flow systems is critical in predicting the flow behavior, pressure drops, and pollutant dispersion in most filtration applications of an industrial or environmental nature. Advanced CFD modeling capabilities enable detailed flow dynamics, turbulence, and stability investigations. In gas-solid hydrodynamic modeling, the choice of drag and viscosity models provides further assurance of accuracy to the predictive results.

This research indicates the critical importance of careful model selection and validation for flow strategy optimization to enhance operational control and efficiency in different scenarios. The basket strainer was designed by CATIA and simulated by ANSYS Fluent. It contains three main parts: Body, cover, and basket, as shown in *Fig. 1*.

The body and cover are constructed from grey cast iron and carbon steel, while the basket is made of stainless steel (304 AISI). The basket strainer operates within a temperature range of -20°C to 100°C.

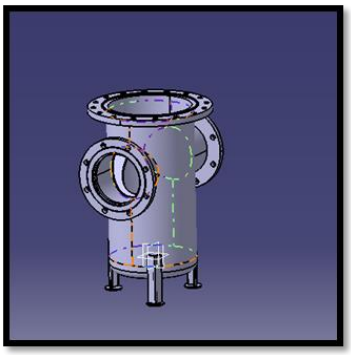

a.

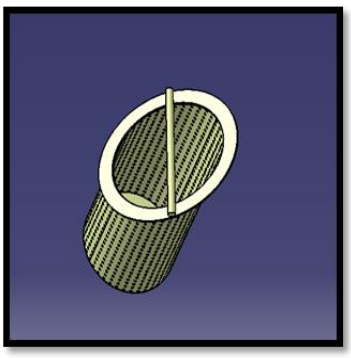

b.

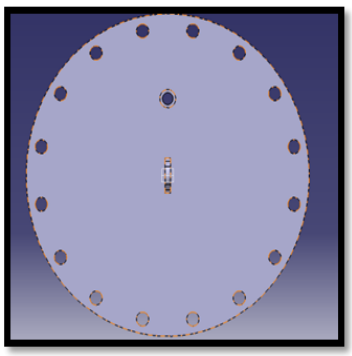

c.

Fig .1. a. Main body; b. strainer; c. cover.

The dimensions of the basket strainer, as shown in *Fig. 2*, include a terminal diameter of 25.4 cm and an inlet diameter of 30.4 cm. The anterior length is 33 cm, while the posterior length is 50.8 cm. Each perforation in the strainer has a diameter of 0.58 cm, enabling efficient filtration while ensuring optimal flow conditions throughout the system. Each of the above features contributes to better performance and functionality of the filtration process.

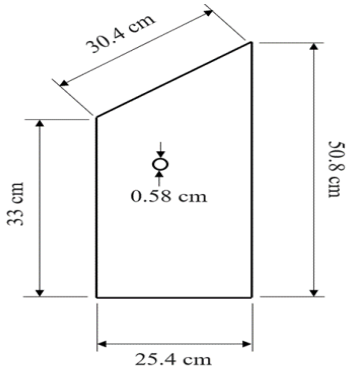

Fig. 2. Basket strainer dimensions.

3.1|Mesh Independency

Meshing was carried out in ANSYS, where the model was discretized into a mix of quadrilateral and triangular elements. The mesh size was adjusted to accurately capture critical areas, particularly regions with high-stress concentrations, ensuring a balance between accuracy and computational efficiency. The total number of elements, approximately one million *Fig. 2*, was modified based on flow rate variations, which served as the criterion for establishing mesh independence.

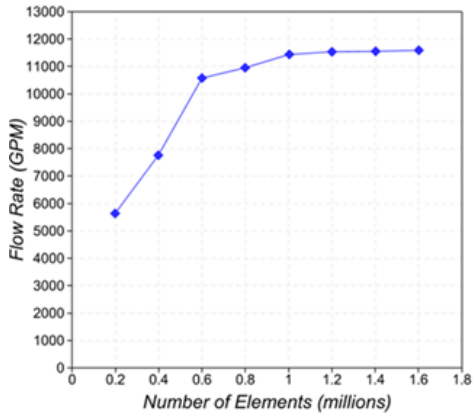

Fig. 3. Mesh independency.

3.2 | Simulation Parameters and Boundary Conditions

The boundary conditions were defined in relation to operational parameters, which included a temperature of 25°C and pressure values for which the inlet pressures range between 0.6 and 20 bar. This is to simulate fluid dynamics in a steady state. The inlet was set as a pressure inlet, while the outlet was designated as the outlet pressure. The significant parameters of operation and the boundary conditions put to use in this simulation are summarized in *Table 1*.

Table 1. Summary of key operational parameters and boundary conditions.

Parameter	Value
Temperature	25°C
Pressure	10^5 Pa
Fluid	Diesel (Liquid)
Fluid density	830 kg/m³
Kinematic viscosity (ν)	5×10^{-6} m²/s
solution type	Pressure-based, steady-state
Turbulence model	k-ε standard
Inlet pressure range	6×10^5 Pa (0.6 bar) to 2×10^6 Pa (20 bar)

4 | Results and Discussion

Recent developments have shown the requirements needed in fluid dynamics and energy optimization in a thermal and filtration system to increase performance. Specific optimization methods, including the use of renewable energy sources, magnetic fields, and optimized flow configurations, have demonstrated effectiveness in reducing operational energy losses while enhancing efficiency in various applications. These approaches show the growing importance of innovative solutions for reduced emissions and sustainable energy goals [27–31].

This section provides a detailed analysis of fluid flow behavior in industrial strainers under varying pressure and flow rate conditions. In particular, basket-type strainers were used in performance testing through diesel and water flows, focusing on the pressure drop and mass flow rate in operation conditions. Numerical simulations, combined with empirical data, were used to compare the results with established theoretical models, with a primary focus on the Darcy-Weisbach equation *Eq. (6)*. The static pressure contour for an inlet pressure of 1 bar is shown in *Fig. 4*.

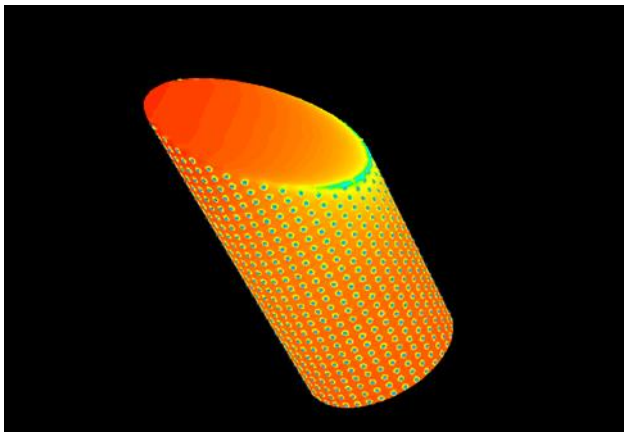

Fig. 4. Contour of static pressure for inlet pressure condition of 1 bar.

4.1 | Diesel Flow Analysis

Since diesel fuel has a higher viscosity than water, it exhibits a high sensitivity to variations in inlet pressure and flow rate. As depicted in *Table 2*, When the inlet pressure increases from 0.6 bar to 20 bar, the mass flow rate and pressure drop also increase accordingly. For example, at an inlet pressure of 6 bar, the pressure drop

across the basket strainer is 5.2 psi, with a corresponding mass flow rate of 3014 GPM. When the inlet pressure is increased to 11 bar, the pressure drop rises to 166 psi, while the mass flow rate simultaneously increases to 18,163 GPM.

Table 2. Results from diesel fluid flow.

Inlet Pressure (Bar)	0.6	1	2	3	4	5	6	7	8	9	10	20
Pressure drop (psi)	5.2	10.1	17	25.5	32.8	42.3	50.7	59	67.3	57.7	84	166
Flow rate (GPM)	3014	4300	5625	6912	8006	9139	9849	10656	11404	12096	12768	18163
Inlet velocity (m/s)	3.5	4.6	6.6	8.1	9.4	10.6	11.6	12.5	13.4	14.2	15	21.3
Outlet velocity (m/s)	8	10.6	15	18.3	21.8	24.4	26.8	29	31	33	34.8	49.5

This comes in line with the Darcy-Weisbach equation, which states that pressure drop (h_f) is directly proportional to the square of velocity (υ). In a system where the cross-sectional area is fixed, an increase in the flow rate instantly raises the velocity and, consequently, the frictional forces acting in the strainer and, therefore, cause a sharp rise in pressure drop. Also, Reynolds number calculations reveal that increasing the flow rate and the inlet pressure changes the flow regime from laminar to turbulent, hence resulting in larger frictional resistance due to a higher pressure drop. The trends shown in *Table 2* are consistent with the conceptual framework introduced through *Eqs. (4)-(6)*; therefore, the model is further validated. *Figs. 5* and *6* present, respectively, diesel flow outlet velocity versus pressure drop and diesel flow pressure drop versus inlet pressure, which demonstrate the above-mentioned trends.

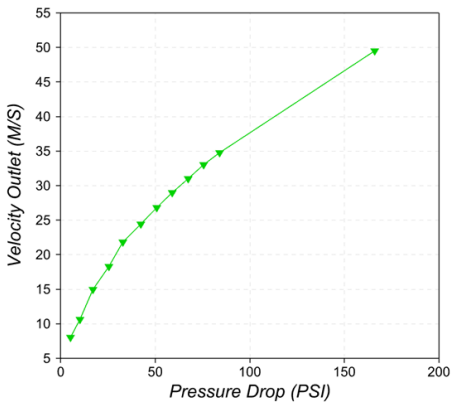

Fig. 5. Velocity outlet against pressure drop of diesel fluid flow.

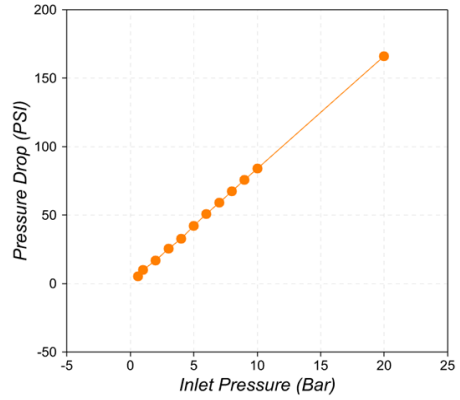

Fig. 6. Pressure drops against inlet pressure of diesel fluid flow.

4.2 | Water Flow Analysis

The analysis of water flow reveals phenomena similar to those observed in diesel flow. However, due to the relatively lower viscosity of water, measured pressure drops are smaller at similar flow rates and pressures.

For example, in *Table 3*, at a flow rate of 500 GPM, the measured pressure drop is only 0.11 psi, with a Reynolds number of 1.6e5—a very near-laminar or transitional flow state. At a flow rate of 10,000 GPM, the pressure drop increases rapidly to 44.94 psi, and the Reynolds number is as high as 3.1e6, which is well into the fully turbulent flow regime. It is observed that the response of water flow to increased flow rates and pressures is consistent with the expected trends described by the Darcy-Weisbach and Hagen-Poiseuille equations, where higher velocity produces larger shear stress and a corresponding increase in pressure loss. This is confirmed by data in *Table 3*, where values closely follow the theoretical descriptions provided in *Eqs. (4)-(6)*.

Table 3. Results from water fluid flow.

Pressure drop (psi)	0.11	0.22	0.36	0.45	1.8	2.81	4.04	7.19	11.24	16.18	22.02	28.76	36.4	44.9
Flow rate (GPM)	500	700	900	1000	2000	2500	3000	4000	5000	6000	7000	8000	9000	10000
Reynolds number	1.6e5	2.2e5	2.8e5	3.1e5	6.3e5	7.9e5	9.4e5	1.2e6	1.5e6	1.9e6	2.2e6	2.5e6	2.8e6	3.1e6
Velocity (m/s)	0.62	0.87	1.12	1.25	2.49	3.11	3.74	4.98	6.23	7.47	8.72	9.96	11.21	12.45

4.3 | Pressure Drop Analysis

The logarithmic relationship between the flow rate and pressure drop is illustrated in *Figs. 7* and *8*, where the pressure drop is shown as a function of the flow rate for diesel and water flow through the basket-type strainer. The plots show an exponential trend, with pressure drops increasing very rapidly as flow rates increase. Logarithmic scaling points out the effect of flow characteristics in the turbulent regime at higher flow rates.

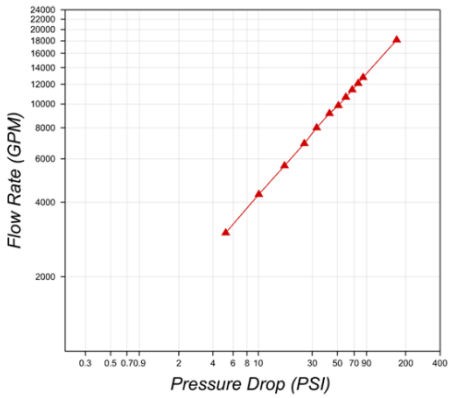

Fig. 7. Flow rate against pressure drop of diesel fluid flow.

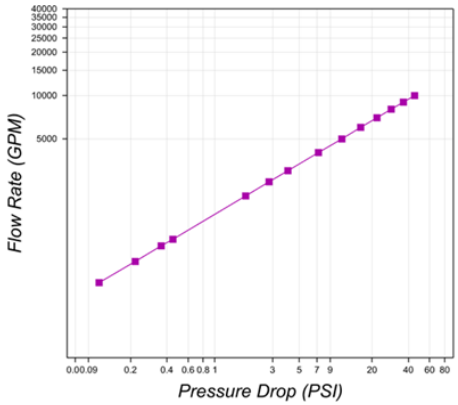

Fig. 8. Pressure drops against inlet pressure of water fluid flow.

4.4 | Model Validation

To demonstrate the predictability of the model, numerical results are compared with measured data obtained for different flow rates between 900 and 5000 GPM for diesel and water. The results reveal good agreement

between numerical results and experimental data [32], an error of less than 10% was noted, as shown in *Fig. 9*. This minor deviation highlights the model's robustness and its capability to capture the underlying fluid dynamics in strainers effectively. The majority of discrepancies can be attributed to simplifications in the computational framework, such as idealized boundary conditions and assumptions of homogeneous material properties, which may not fully reflect the physical complexities of real-world strainer systems.

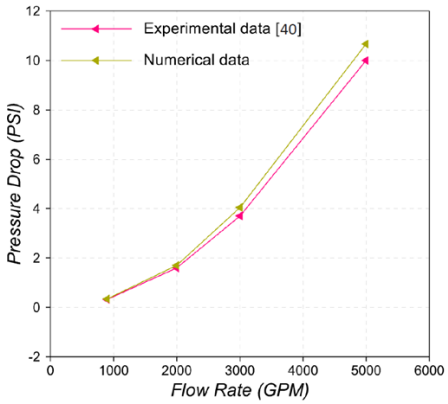

Fig. 9. Theoretical and experimental comparisons for water.

The margin of error also depends on the actual surface roughness and porosity of strainers and slight manufacturing process variations, which are not easy to reproduce faithfully in a simulation environment. However, the good agreement between simulation and empirical evidence supports the confidence in the computational model to predict fluid dynamics for industrial strainer applications accurately.

6 | Conclusion

This study presents numerical modeling and analysis of pressure drop and flow behavior in industrial basket strainers, which are critical for enhancing filtration efficiency in hydraulic systems. Numerical simulations combined with empirical validation show that variations in inlet pressure, flow rate, and fluid properties, particularly the higher viscosity of diesel, result in significantly greater pressure drops compared to water under similar conditions.

For example, diesel inlet pressure from 0.6 to 20 bar increased the pressure drop from 5.2 psi to 166 psi and the mass flow rate from 3014 to 18163 GPM. The flow of water also showed similar trends but with lower pressure drops, clearly emphasizing the influence of fluid property on the flow behavior. Validated against empirical data within an approximate error margin of 10%, the developed computational model was effective in predicting pressure reduction and flow behavior in agreement with applicable theoretical frameworks, including the Darcy-Weisbach equation. Especially, the pressure drops of the turbulent flow at high rates were considerably increased, further proving the importance of optimized strainer configurations for the minimization of potential energy losses and improvement of equipment life.

These research findings demonstratively show the importance of careful strainer design and continuous flow monitoring in the improvement of filtration efficiency, reduction in operational costs, and extension in the service life of fluid machines. This validated modeling approach constitutes a strong tool for fluid dynamics prediction concretely aiming at improvements in industrial filtration and system effectiveness.

Funding

This research did not receive any specific grant from funding agencies in the public, commercial, or not-for-profit sectors.

Data Availability

The data that support the findings of this study are available from the corresponding author upon reasonable request.

Conflicts of Interest

The authors declare no conflicts of interest related to this work.

References

[1] Hosseini, H., Mozaffari, A., Khodabandeh, Z., & Kia, S. (2024). Evaluation of Ammonia as a replacement for water in surface condensers: Performance and efficiency. *Journal of environmental engineering and energy*, *1*(1), 47–58. https://doi.org/10.22105/jeee.v1i1.29

[2] Khodabandeh, Z., Kia, S., Aminipour, F., Mozaffari, A., Hosseini, H., & Jahangiri, A. (2024). Exergy-driven optimization of Ammonia as a sustainable cooling agent for water-constrained power Systems. *Journal of environmental engineering and energy*, *1*(1), 71–82. https://doi.org/10.22105/jeee.v1i1.27

[3] Kia, S., Khodabandeh, Z., Barani, A., & Aminipour, F. (2024). Technical feasibility of exhaust heat recovery in reciprocating engines: A case study on power generation systems. *Journal of environmental engineering and energy*, *1*(1), 83–93. https://doi.org/10.22105/jeee.v1i1.28

[4] Kia, S., Khanmohammadi, S., & Jahangiri, A. (2023). Experimental and numerical investigation on heat transfer and pressure drop of SiO2 and Al2O3 oil-based nanofluid characteristics through the different helical tubes under constant heat fluxes. *International journal of thermal sciences*, *185*, 108082. https://doi.org/10.1016/j.ijthermalsci.2022.108082

[5] Ashrafi, N., Sadeghi, A., & others. (2018). Numerical simulation of visco-plastic fluid flow between two parallel plates with triangular obstacles. *Bulletin of the american physical society*, *63*(13). https://meetings.aps.org/Meeting/DFD18/Event/334178

[6] Catalano, P., Wang, M., Iaccarino, G., & Moin, P. (2003). Numerical simulation of the flow around a circular cylinder at high Reynolds numbers. *International journal of heat and fluid flow*, *24*(4), 463–469. https://doi.org/10.1016/S0142-727X(03)00061-4

[7] Ikpe, A. E., Ekanem, I., & Ekanem, K. R. (2024). Conventional trends on carbon capture and storage in the 21st century: a framework for environmental sustainability. *Journal of environmental engineering and energy*, *1*(1), 1–15. https://B2n.ir/jh9630

[8] Wilson, E. O., Charles. O. A., & Jerry, E. P.. (2024). Temperature effects on the corrosion inhibition of mild steel in crude oil medium by the seed extract of Persea Americana (Avocado Tree). *Journal of environmental engineering and energy*, *1*(1), 16–23. https://doi.org/10.22105/jeee.v1i1.21

[9] Bazdidi-Tehrani, F., Ebrahimi, A., & Azimi-Souran, R. (2024). Investigation of forced convection of a novel hybrid nanofluid containing NEPCM in a square microchannel: Application of single-phase and Eulerian-Eulerian two-phase models. *Numerical heat transfer, part a: applications*, *86*(11), 1–22. https://doi.org/10.1080/10407782.2024.2305231

[10] Ubabuike, U. H., Ime, J. U., Anosike, A. C., & Wilson, E. O. (2024). Comparative performance study of kolanut biodiesel and conventional fossil diesel. *Journal of environmental engineering and energy*, *1*(1), 24–31. https://doi.org/10.22105/jeee.v1i1.23

[11] Arshizadeh, S., Khanmohammadi, S., Jahangiri, A., Sajedi, S. M. H., Panchal, H., Prakash, C., & Gupta, N. K. (2024). Thermodynamic modeling and multi-objective optimization of an operating double-effect absorption chiller driven by photovoltaic panel: A case study. *Journal of environmental engineering and energy*, *1*(1), 32–46. https://B2n.ir/se9970

[12] Graciano-Uribe, J., Pujol, T., Puig-Bargués, J., Duran-Ros, M., Arbat, G., & de Cartagena, F. (2021). Assessment of different pressure drop-flow rate equations in a pressurized porous media filter for irrigation systems. *Water*, *13*(16), 2179. https://doi.org/10.3390/w13162179

[13] Korkmaz, Y. S., Kibar, A., & Yigit, K. S. (2022). Experimental and numerical investigation of fluid flow in hydraulic filters. *Journal of applied fluid mechanics*, *15*(2), 363–371. https://doi.org/10.47176/jafm.15.02.32898

[14] Brazhenko, V., Qiu, Y., Mochalin, I., Zhu, G., Cai, J. C., & Wang, D. (2022). Study of hydraulic oil filtration process from solid admixtures using rotating perforated cylinder. *Journal of the taiwan institute of chemical engineers*, *141*, 104578. https://doi.org/10.1016/j.jtice.2022.104578

[15] Klarecki, K., & Rabsztyn, D. (2019). Experimental verification of the filtration phenomena in hydraulic systems. *Mechatronics 2017-ideas for industrial applications 4* (pp. 220–230). Springer. https://doi.org/10.1007/978-3-030-15857-6_22

[16] Tič, V., & Lovrec, D. (2021). Pressure drop development on hydraulic filter as an on-line condition monitoring indicator. *International conference "new technologies, development and applications"* (pp. 781–787). Springer. https://doi.org/10.1007/978-3-030-75275-0_86

[17] Gorle, J. M. R., Heiskanen, V. M., Nissi, S., & Majas, M. (2018). Effect of temperature, flow rate and contamination on hydraulic filtration. *MM science journal*, *2018*, 2490–2493. 10.17973/MMSJ.2018_10_201852

[18] Sperone, G. (2023). Homogenization of the steady-state Navier-Stokes equations with prescribed flux rate or pressure drop in a perforated pipe. *Journal of differential equations*, *375*, 653–681. https://doi.org/10.1016/j.jde.2023.08.033

[19] Gaj, N., & Madramootoo, C. A. (2021). Structural response of non-perforated and perforated corrugated high-density polyethylene pipes under variable loading. *Biosystems engineering*, *207*, 120–140. https://doi.org/10.1016/j.biosystemseng.2021.05.002

[20] Mahajan, G., & Maurya, R. S. (2020). Development of an efficient t-type strainer with its performance evaluation. *Journal of thermal engineering*, *6*(6), 420–433. https://doi.org/10.18186/thermal.836499

[21] Neihguk, D., Munjal, M. L., & Prasad, A. (2015). *Pressure drop characteristics of perforated pipes with particular application to the concentric tube resonator* (No. 2015-01-2309). SAE Technical Paper. https://doi.org/10.4271/2015-01-2309

[22] Azadi, M., Aminossadati, S. M., & Chen, Z. (2017). Development of an integrated reservoir-wellbore model to examine the hydrodynamic behaviour of perforated pipes. *Journal of petroleum science and engineering*, *156*, 269–281. https://doi.org/10.1016/j.petrol.2017.05.027

[23] Afifi, M. D., Jahangiri, A., & Ameri, M. (2025). Investigation of natural convection heat transfer in MHD fluid within a hexagonal cavity with circular obstacles. *International journal of thermofluids*, *25*, 101024. https://doi.org/10.1016/j.ijft.2024.101024

[24] Mirzaei, A., Jalili, P., Afifi, M. D., Jalili, B., & Ganji, D. D. (2023). Convection heat transfer of MHD fluid flow in the circular cavity with various obstacles: Finite element approach. *International journal of thermofluids*, *20*, 100522. https://doi.org/10.1016/j.ijft.2023.100522

[25] Dehghan Afifi, M., Jalili, B., Mirzaei, A., Jalili, P., & Ganji, D. (2025). The effects of thermal radiation, thermal conductivity, and variable viscosity on ferrofluid in porous medium under magnetic field. *World journal of engineering*, *22*(1), 218–231. https://doi.org/10.1108/WJE-09-2023-0402

[26] Jalili, P., Afifi, M. D., Jalili, B., Mirzaei, A. M., & Ganji, D. D. (2023). Numerical study and comparison of two-dimensional ferrofluid flow in semi-porous channel under magnetic field. *International journal of engineering*, *36*(11), 2087–2101. https://B2n.ir/rj5409

[27] Dehghan Afifi, M., Jahangiri, A., & Ameri, M. (2025). Numerical and analytical investigation of Jeffrey nanofluid convective flow in magnetic field by FEM and AGM. *International journal of thermofluids*, *25*, 100999. https://doi.org/10.1016/j.ijft.2024.100999

[28] Jahangiri, A., Ameri, M., Arshizadeh, S., & Alvari, Y. (2023). District heating and cooling for building energy flexibility. In *Building energy flexibility and demand management* (pp. 173–190). Elsevier. https://doi.org/10.1016/B978-0-323-99588-7.00008-0

[29] Dezfouli, A. H. M., Arshizadeh, S., Bakhshayesh, M. N., Jahangiri, A., & Ahrari, S. (2024). The 4E emergy-based analysis of a novel multi-generation geothermal cycle using LNG cold energy recovery. *Renewable energy*, *223*, 120084. https://doi.org/10.1016/j.renene.2024.120084

[30] Hosseinizadeh, S. E., Majidi, S., Goharkhah, M., & Jahangiri, A. (2021). Energy and exergy analysis of ferrofluid flow in a triple tube heat exchanger under the influence of an external magnetic field. *Thermal science and engineering progress*, *25*, 101019. https://doi.org/10.1016/j.tsep.2021.101019

[31] Okafor, C. J. (2024). Energy generation in Nigeria: A literature review. *Journal of environmental engineering and energy*, *1*(1), 59–70. https://B2n.ir/zd7038

[32] Company, K. (2012). *Style A Y-strainer: Technical and application information*. https://B2n.ir/qp4379